Supplement:

Materials and Methods

Reporter cell line. The full-length human *MECP2-e2* coding sequence was cloned into pLenti-Global Protein Stability (GPS) (*37, 38*) to generate Dsred-IRES-MECP2-EGFP with the selection modified to NeoR. Lentivirus was used to infect Daoy cells at a low multiplicity of infection (0.3) to promote single copy integration. Cells carrying the transgene were then selected by geneticin (500 μg/mL) and clones obtained by fluorescence-activated cell sorting (FACS) using an Aria II cell sorter (BD Biosciences) of single double-positive (DsRed and EGFP) cells into individual wells.

Cell-based RNAi screen by flow cytometry. The screen was carried out with kinase and phosphatase siRNA libraries from Invitrogen. Reporter cells were plated in 96-well plates and transfections were performed in triplicate across three independent plates. Each plate included three scrambled siRNAs serving as internal negative controls. 72 hours post-transfection, flow cytometric analysis of cells was performed on a LSRII Fortessa coupled with a High Throughput Sampler (HTS) module (BD Biosciences). Gates for analysis were set using single-positive and double-positive cells as well as negative cells. The GFP/DsRed ratio was determined for each sample and normalized by the on-plate scrambled siRNA controls. Multiple comparisons corrected t-tests were used to identify hits using a *P*-value cut-off of <0.01. Top hits from each screen met the *P*-value cut-off and had more than two siRNAs with a significant effect. The secondary screen was performed exactly the same way but with independent siRNAs (Stealth siRNAs, Invitrogen). Further validation utilized shRNAs from the human pGIPz collection (ThermoScientific).

Gene expression analysis. Total RNA from cultured cells and mouse brain tissue was extracted using miRNeasy minikit (Qiagen) and Aurum Total RNA Fatty and Fibrous Tissue Kit (Bio-Rad), respectively. cDNA was generated from 1.5 µg of total RNA by reverse transcription with the Moloney Murine Leukemia Virus (M-MLV) system (Invitrogen) and random hexamer priming. RT-qPCR was performed in a CFX96 Real-Time System (Bio-Rad) using PerfeCTa SYBR Green Fast Mix (Quanta Biosciences). Sense and antisense primers were selected to be located on different exons. The specificity of the amplification products was verified by melting curve analysis. All RT-qPCR reactions were conducted in technical triplicates and the results were averaged for each sample, normalized to *GAPDH* levels, and analyzed using the comparative ddCt method. Primers are listed in table S2.

Vectors. pGIPZ clones (Open Biosystems) used and their shRNA sequences are listed in table S3. For *in vivo Ppp2r1a* knockdown, scrambled and TRCN0000012624 (The RNAi Consortium) shRNAs were cloned into the miR30 cassette of pAAV-U6-miR-Cag-tdT (table S3). Mouse *Hipk2* (MGC CloneId: 5368577) and *Hipk1* (MGC CloneId: 40131000) cDNAs were subcloned into pcDNA3.1. For the generation of doxycycline-inducible transgenic cell lines full-length human *MECP2-e2* coding sequence followed by a C-terminal GFP tag was cloned into pINDUCER20 (*70*).

In vitro kinase assays. Recombinant human MeCP2 was purified as previously reported (*71*). For radioactive assays, 3 ug of MeCP2 with chitin-binding protein (CBP) C-terminally fused was incubated with 100 ng recombinant HIPK1 (Thermo Fisher Scientific PV4561) or HIPK2

(Thermo Fisher Scientific PV5275) in 15 mM HEPES pH 7.5, 10 mM $MgCl_2$, 50 mM ATP, and 8 uCi γ-^{32}P[ATP] for 30 min at 30°C. To demonstrate the specificity of the radioactive-phosphate labeling, the chitin resin binding MeCP2-CBP from an aliquot of the reaction was washed. Cold reactions for mass spectrometric analyses, reactions were performed as above, but scaled up to 10 ug of MeCP2-CBP along with 1ug kinase and incubated for 2 hours. RIOK1 reactions were performed as described (*42*). Human RIOK1-6His was purified from TNT® Quick Coupled Transcription/Translation Systems (Promega) reactions with the MagZ™ Protein Purification System.

Mass spectrometry analysis. MeCP2 bands were excised from Coomassie-stained SDS-PAGE gels, destained and subject to in-gel digestion using 100 ng of trypsin (GenDepot T9600). The tryptic peptide was resuspended in 10µl of 0.1% formic acid and subjected to nanoHPLC-MS/MS system consisted with a Ultimate 3000 HPLC coupled to Fusion Tribrid Orbitrap™ (Thermo Scietific) mass spectrometer. The peptides were loaded onto a Reprosil-Pur Basic C18 (1.9 µm, Dr.Maisch GmbH, Germany) precolumn of 2cm X 100µm size. The precolumn was switched in-line with an in-housed 50 mm x 150 um analytical column packed with Reprosil-Pur Basic C18 equilibrated in 0.1% formic acid. The petides were eluted using a 75min discontinuous gradient of 4-26% acetonitrile/0.1% formic acid at a flow rate of 600nl/min. The eluted peptides were directly electro-sprayed into mass spectrometer operated in the data-dependant acquisition mode acquiring fragmentation spectra of the top 50 strongest ions. Obtained MS/MS spectra were searched against target-decoy human refseq database in Proteome Discoverer 1.4 interface (Thermo Fisher) with Mascot algorithm (Mascot 2.4, Matrix Science). The precursor mass tolerance was confined within 20 ppm with fragment mass tolerance of 0.5

dalton and a maximum of four missed cleavage allowed. Dynamic modification of phosphorylation on serine, threonine and tyrosine was allowed, together with oxidation (methionine), protein N-terminal acetylation and destreak (cysteine). The peptides identified from mascot result file were validated with 5% false discover rate (FDR) and subject to manual verifications. For relative quantification of phosphorylation, raw spectrum file was crunched to .mgf format by PD1.4 and then imported to Skyline with raw data file. Transition list generation and data analysis are performed by SKYLINE™ software. The specific combination of peptide mass and product ions masses constitute the identity of the target peptide. The peak areas under the curves of target peptides reveal the quantity of the target peptides in the sample.

Immunoprecipitations. Human MeCP2-EGFP was immunoprecipitated from the lysate of three pooled whole brains of transgenic male mice (*19*) null for the mouse allele (*MECP2-EGFP*^{Tg}*; Mecp2−/y*). The brains were Dounce homogenized in 5 volumes of NETN buffer (50 mM Tris-HCl pH 7.3, 170 mM NaCl, 1 mM EDTA, 0.5% NP40) with protease and phosphatase inhibitors. After centrifugation at 1000 *g* for 4 min at 4°C, the cytosolic supernatant was removed and the pellet resuspended in 2 volumes of NETN. Following sonication (2 30s 20% cycles), lysates were spun at 10,000 *g* for 10 min at 4°C. The nucleoplasmic supernatant was removed and the pellet solubilized by sonication (12 15s 20% cycles) in one volume of RIPA buffer (50 mM Tris-HCl pH 8.0, 150 mM NaCl, 1% NP-40, 0.5% sodium deoxycholate, 0.1% SDS). Following ultracentrifugation at 200,000 *g* for 20 min at 4°C, the supernatant of solubilized chromatin was applied to 50 µl of GFPTrap (Bulldog Bio) bead slurry (50%). Samples were rotated for 1 hour at 4°C. Beads were washed 3 times with NETN buffer then boiled in Laemmli buffer. Cell culture immunoprecipitations were performed as reported (*71*). Briefly, 48 h after transfection for

HEK293T or after drug treatment for transgenic Daoy, cells were collected in ice-cold PBS and pelleted in a tabletop centrifuge. Cells were lysed by rotation in 500 ul of ice-cold cell lysis buffer (20 mM Tris-HCl pH 8.0, 180 mM NaCl, 1 mM EDTA, 0.5% NP-40, and Complete protease inhibitor (Roche)) for 20 min. The lysate was cleared by spinning at 15,000 *g* for 15 min at 4°C. The cleared lysate (input) was added to protein A-Dynabeads (Life Technologies) saturated with rabbit anti-GFP serum (Abcam ab290). Samples were rotated for 1 hour at 4°C. Beads were then washed four times in cell lysis buffer, and bound complexes were eluted by boiling in Laemmli.

Viral generation. Lentiviral vectors and their packaging vectors psPAX2 and pMD2G were cotransfected in a 4:3:1 molar ratio into HEK293T cells. Media was collected at 48 h following transfection, replaced with fresh media (5 mL) and collected again at 72 h. Viral supernatant was cleared from cell debris via centrifugation (10 min at 4,000 rpm) as well as filtration through a 0.45 μM polyethersulfone membrane (VWR). AAV8 bearing pAAV-U6-miR-Cag-tdT was generated by the Baylor College of Medicine DNA Sequencing and Gene Vector Core with a titer of ~10^{13} genome copies/ml.

Mice. To overcome issues related to a pure inbred strain, we generated F1 hybrid animals by mating FVB/N *MECP2*^{TG1}(*7*) females to wild-type C57Bl/6 males obtained from Jackson Laboratories). Littermates were used as controls in all experiments. Mice were maintained in a temperature-controlled, AAALAS-certified Level 3 facility on a 12 hr light-dark cycle. Food and water were given *ad libitum*. All procedures to maintain and use these mice were approved by the Institutional Animal Care and Use Committee for Baylor College of Medicine.

Chemicals. Okadaic acid (sc-3513) was obtained from Santa Cruz Biotechnology. Fostriecin was obtained from Santa Cruz Biotechnology (sc-202160) for cultured neuron experiments and from Sigma-Aldrich (F4425) for *in vivo* injections. For experiments in which a shared solvent control was used, both drugs were dissolved in methanol, a solvent acceptable for both. On all other occasions the drugs were dissolved in their optimal solvent (DMSO for okadaic acid and sterile saline for fostriecin) and that vehicle used as the control. For *in vivo* injections, only freshly dissolved fostriecin was used to ensure potency.

Primary neuron culture. Primary cerebellar granule precursors were generated as previously described (*72*) with slight modifications. Briefly, cerebella from P5-P9 mice were dissected and dissociated with trypsin. Granule neurons were specifically isolated using a percoll gradient following which single cell suspensions were plated onto 24-well plates coated with poly-L-lysine.

Intracerebral injections. P0 intraventricular injections were performed as described (*73*). Viral stocks were diluted in PBS to equivalent concentrations and 2 ul injected into each ventricle, delivering 2 x 10^{10} AAV8 viral particles/hemisphere. For adult injections with okadaic acid, mice were injected with 5 ul of 8 ng/ul okadaic acid dissolved with 2% DMSO in sterile saline or vehicle largely as previously reported (*30*). For fostriecin injections, 5 ul of 240 uM (unless otherwise specified) fostriecin freshly dissolved in sterile saline was used, with saline as the vehicle control. Briefly, mice were anaesthetized with isoflurane and placed on a computer-guided stereotaxic instrument (Angle Two Stereotaxic Instrument, Leica Microsystems).

Isoflurane (3%) was continuously delivered via a small face mask. Ketoprofen (5 mg/kg) was administered subcutaneously at the initiation of surgery. After sterilizing the surgical site, a midline incision was made over the skull and a small hole was drilled through the skull above the right lateral ventricle. A total of 5 ul was delivered using a Hamilton syringe connected to a motorized nanoinjector at 166 nl/s. The coordinates used relative to bregma were as follows: anteroposterior (AP) = + 0.3 mm, medial lateral (ML) = 1 mm, dorsal ventral (DV) = − 3 mm. To allow diffusion of the solution into the brain, the needle was left for three min on the site of injection. The incision was manually closed with suture. Carprofen-containing food pellets were provided for three days after the surgery.

Accelerating rotating rod (rotarod). Mice were habituated in the test room (550 lx, 60 dB white noise) for 30 min. Motor coordination was measured using an accelerating rotarod apparatus (Ugo Basile, Varese, Italy). Mice were tested for 2 consecutive days, 4 trials each, with an interval of 60 min between trials to rest. Each trial lasted for a maximum of 10 min and the rod accelerated from 4 to 40 r.p.m. in the first 5 min. The time that it took for each mouse to fall from the rod (latency to fall) was recorded.

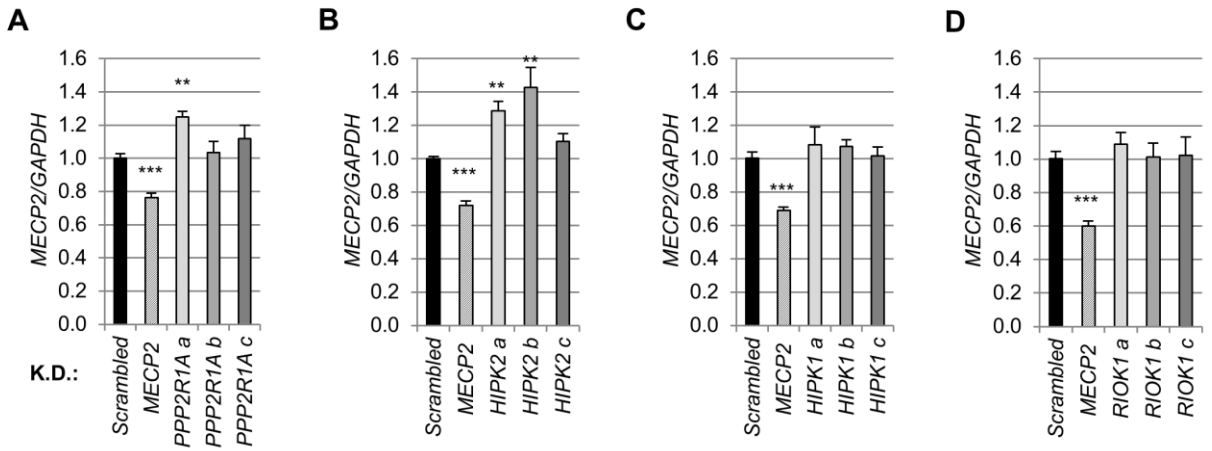

Fig. S1. Candidate knockdown did not decrease *MECP2* transcript levels. For each candidate, HEK293T cells were transfected with three shRNAs (a-c) along with vectors expressing scrambled shRNA and shRNA targeting *MECP2*. Two days post-transfection, puromycin was applied for four days to select for cells expressing the silencing plasmid. **(A)** The effects of *Protein Phosphatase 2 Regulatory subunit 1 Alpha* (*PPP2R1A*) knockdown on *MECP2* transcript levels relative to *GAPDH*. Despite significant decreases in MeCP2 protein levels (Fig. 2A) with shRNAs "a" and "c," which resulted in significant knockdown of *PPP2R1A*, *MECP2* transcript levels were not significantly decreased. **(B)** As in **A**, but for *Homeodomain Interacting Protein Kinase 2* (*HIPK2*). **(C)** As in **A** and **B**, but for *Homeodomain Interacting Protein Kinase 1* (*HIPK1*). **(D)** As in **A**-**C**, but for *RIO Kinase 1* (*RIOK1*). K.D., knockdown. Values are mean ± s.e.m., n = 3-4 per group. **p<0.01; ***p<0.001, two-tailed *t*-test.

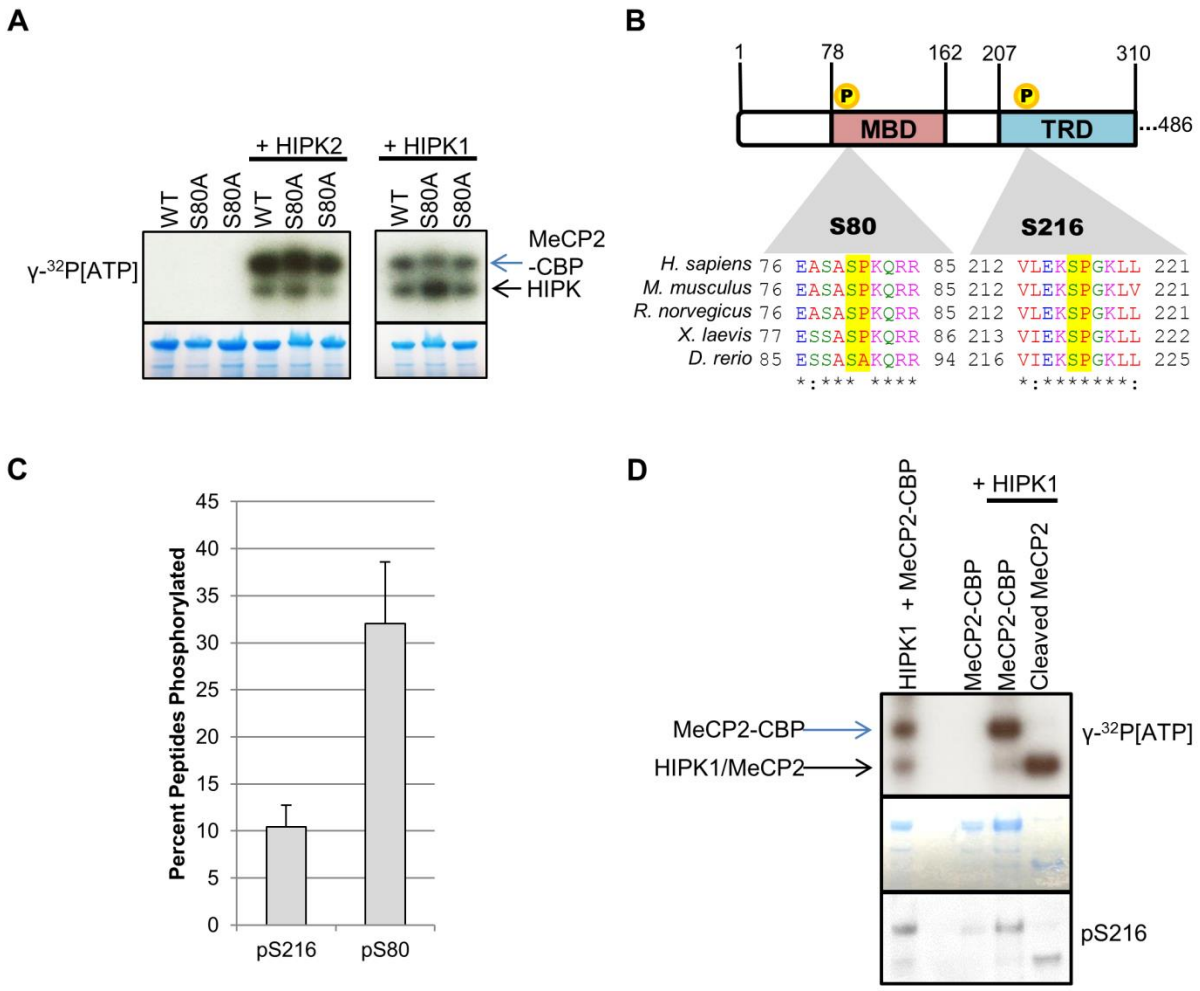

Fig. S2. MeCP2 pS16 occurred *in vivo*. **(A)** Autoradiogram (top) and Coomassie-stained gel (bottom) of radioactive kinase reactions with either HIPK2 or HIPK1 as kinase and CBP-tagged wild-type MeCP2 (WT) or MeCP2 that could not be phosphorylated at S80 (S80A) provided as substrate. Radioactive phosphate incorporation did not appear to decrease when MeCP2 could not be phosphorylated at S80. n = 3. **(B)** The domain location and conservation of HIPK phosphosites, S80 and S216. The two defined domains of MeCP2, the methyl-CpG binding domain (MBD) and the transcriptional repression domain (TRD), are depicted with numbering relative to the human MeCP2-e2 isoform. S80 falls at the N-terminal edge of the MBD, whereas S216 lies within the TRD. Both S80 and S216 are highly conserved from zebrafish to human.

Orthologs were aligned using Clustal Omega. The HIPK consensus site is highlighted. *, fully conserved. :, highly similar amino acid properties. **(C)** Immunoprecipitation of human MeCP2-EGFP from whole brain followed by tandem mass spectrometry revealed the occurrence of pS216 *in vivo*. Percent peptide phosphorylated relative to the sum of modified and unmodified peptides for peptides containing S216 (or pS80 for internal reference). Area under the peptide curves was utilized for relative quantitation. The pooled lysate of three whole brains was used per experiment. n = 2. **(D)** Fig. 3B kinase reactions probed for pS216. Autoradiogram (top) and Coomassie-stained gel (bottom) of kinase reaction with the indicated recombinant proteins in the presence of γ-^{32}P[ATP]. Incubation of HIPK1 and MeCP2-CBP resulted in HIPK1 autophosphorylation and phosphorylation of MeCP2 (lane 1). Whereas MeCP2-CBP without HIPK1 resulted in no detectable radioactivity (lane 3). To control for epitope phosphorylation, chitin-bound MeCP2-CBP incubated with HIPK1 was washed (lane 4) then eluted by tag cleavage (lane 5). n = 3.

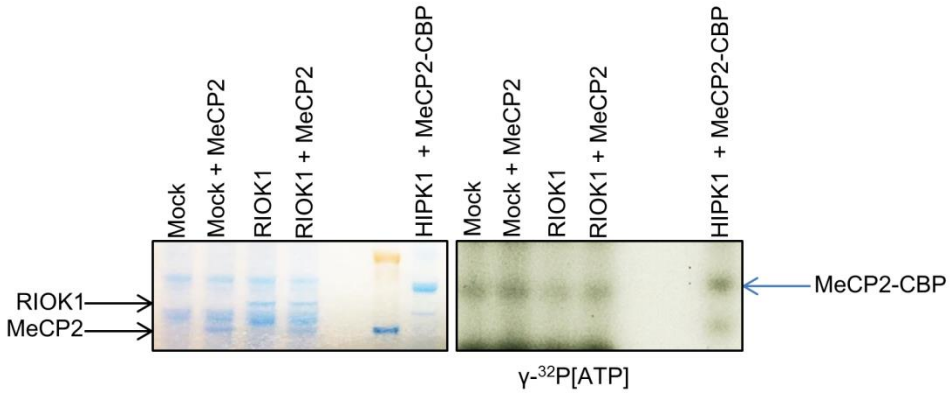

Fig. S3. No RIOK1 kinase activity for MeCP2 was detected. Nickel-purified lysates from rabbit reticulocyte transcription and translation reactions with no vector (Mock) or RIOK1-6His were incubated with recombinant MeCP2 in the presence of γ-^{32}P[ATP]. As a positive control, a similar reaction with MeCP2-CBP and recombinant HIPK1 was performed in parallel. Coomassie-stained gel (left), autoradiogram (right). n = 3.

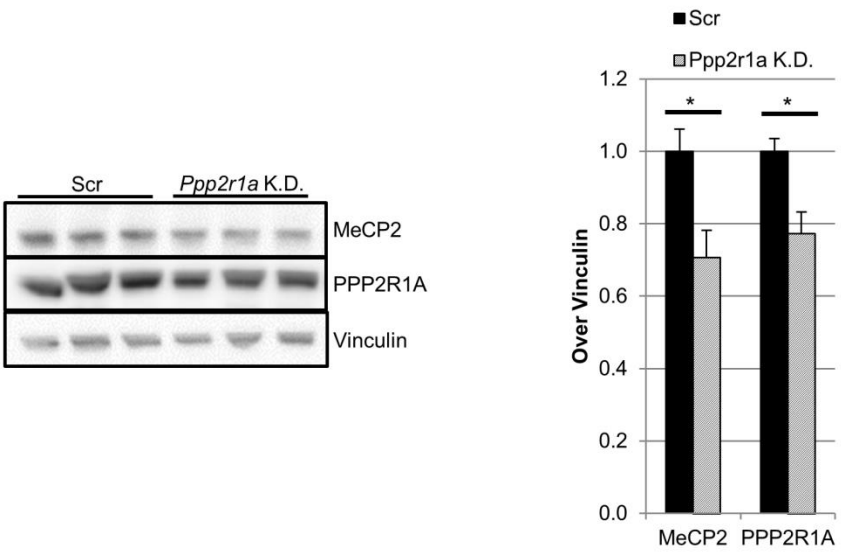

Fig. S4. *Ppp2r1a* knockdown also decreased MeCP2 levels in hippocampal tissue. Independent P0 intraventricular injections of AAV8 encoding shRNA targeting *Ppp2r1a* were performed to determine if *Ppp2r1a* knockdown decreased MeCP2 levels in hippocampi. PPP2R1A regulation was not specific to cortical tissue, as MeCP2 levels were also decreased in hippocampal lysates compared to animals injected with virus expressing a scrambled shRNA. Hippocampal tissue was harvested two weeks post-injection. n = 3. Values are mean ± s.e.m., *p< 0.05, two-tailed *t*-test.

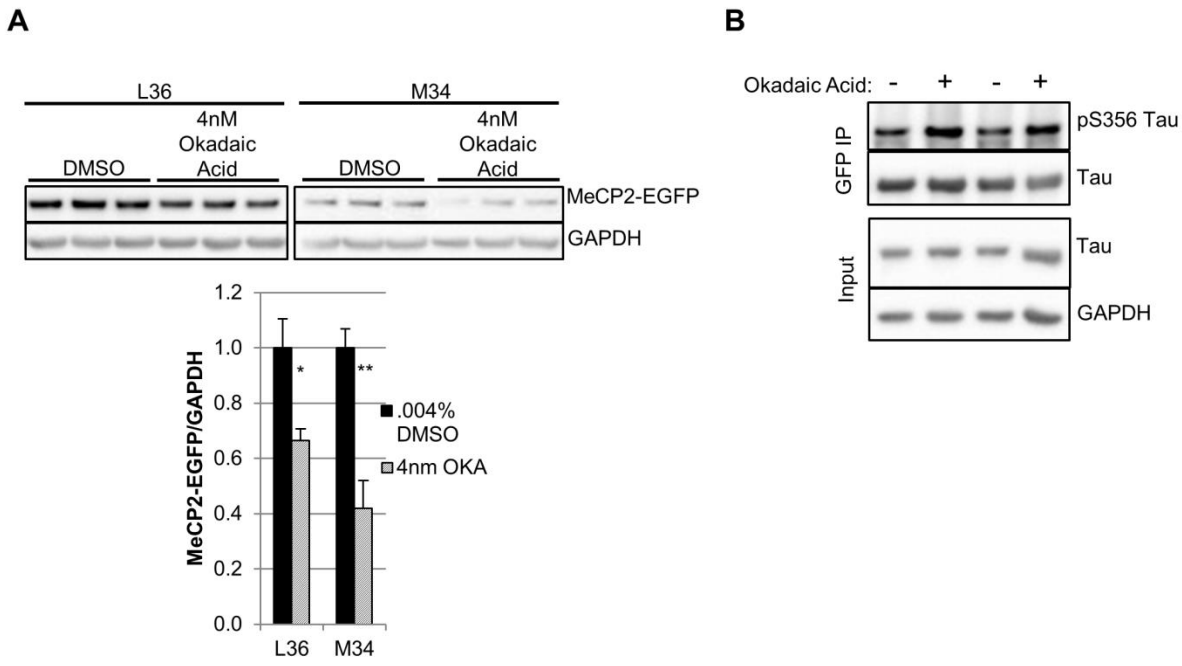

Fig. S5. Okadaic acid treatment was active against human MeCP2. **(A)** Two unique Daoy *MECP2-EGFP* transgenic clones (L36 and M34) were treated with 0.004% DMSO or 4 nM okadaic acid (OKA) and the amount of MeCP2 detected after eight days of treatment. n = 3 per group. Values are mean ± s.e.m., *p<0.05; **p<0.01, two-tailed *t*-test. **(B)** To control for the efficacy of our pharmacological inhibition, the phosphorylation status of the PP2A substrate Tau was analyzed. We utilized a stabile Tau-EGFP Daoy cell line (Lasagana-Reeves et al., *Neuron*, 2016) from which we could immunoprecipitate Tau for increased sensitivity to changes in phosphorylation. Using the same concentration of okadaic acid which was effective in decreasing MeCP2-EGFP in Daoy (4 nM), we observed increased levels of pS356 relative to total tau levels after eight days of treatment. Thus, we were able to determine that the same PP2A inhibition regimen effective in decreasing MeCP2, resulted in the anticipated increase in its substrate Tau pS356 (Kickstein et al., *PNAS* 2010). n = 3.

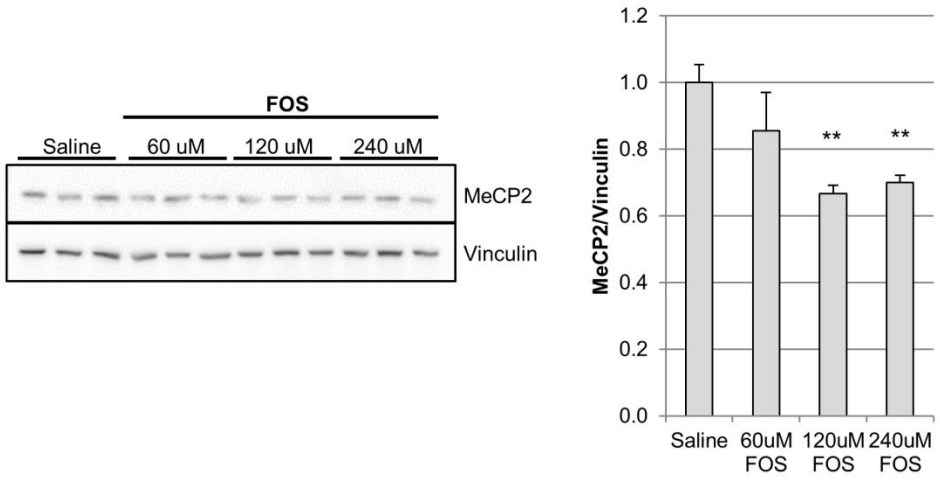

Fig. S6. *In vivo* fostriecin titration. The effect on cortical MeCP2 levels of increasing doses of fostriecin (FOS) was determined by intraventricular injection followed by immunoblotting. Compared to mice injected with solvent (Saline) alone, mice injected with 120 uM and 240 uM FOS exhibited significant decreases in MeCP2. Cortices were harvested one week post-injection. n = 3 - 6. Values are mean ± s.e.m., **p<0.01, two-tailed *t*-test.

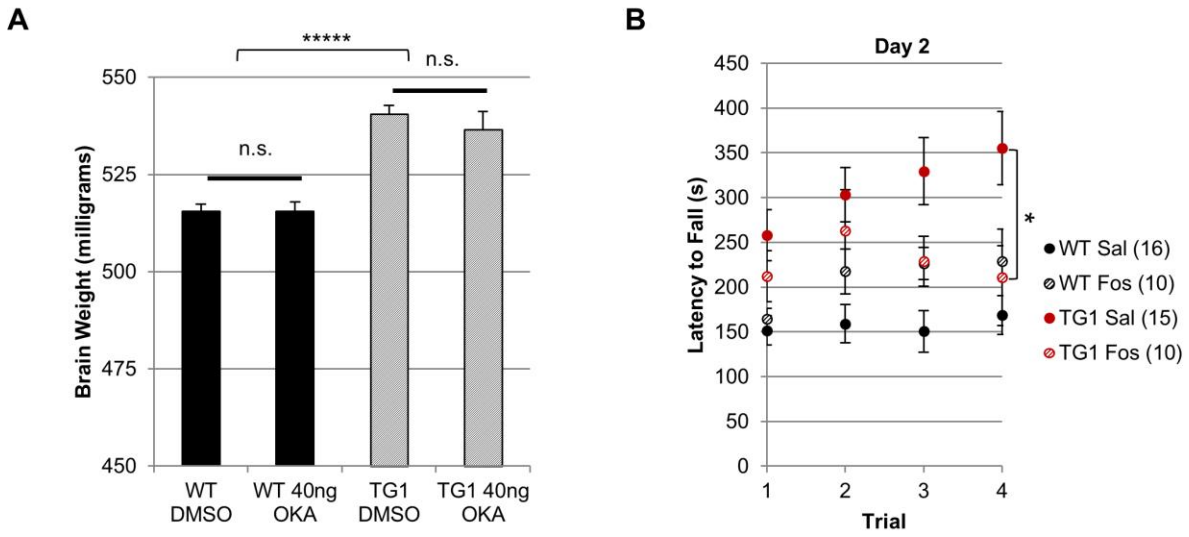

Fig. S7. *In vivo* PP2A inhibition resulted in no ill effects in WT at the doses used. **(A)** Healthy brain weights maintained in mice injected with okadaic acid. Total brain weights two weeks post-injection of mice intraventricularly injected with 2% DMSO or 40 ng of okadaic acid (OKA) did not significantly differ, regardless of genotype. Interestingly, *MECP2*^{TG1} mice, mice expressing both mouse *Mecp2* and human *MECP2* such that twice the MeCP2 protein is expressed, displayed significantly increased brain weight compared to wild-type littermates. n = 12, n = 14, n = 13, and n = 15 for WT DMSO, WT 40ng, TG1 DMSO, and TG1 40ng, respectively. **(B)** Fostriecin (Fos) treatment of *MECP2*^{TG1}mice partially rescued abnormal motor persistence on the accelerating rotating rod as evidenced by decreased latency to fall compared to *MECP2*^{TG1}mice treated with saline alone (Sal), whereas no decreased occurred in WT treated with Fos. Mice were assessed two weeks post-injection. n = 10-16, as indicated in parentheses. Values are mean ± s.e.m., *p< 0.05, *****p<10^{-6} A, two-tailed *t*-test. B, repeated-measures two-way analysis of variance (ANOVA) by day followed with post hoc *t*-tests.

Table S1. MeCP2-specific siRNAs gene list.

Gene	MeCP2-specific siRNAs
ACVR2B	2
ALDH18A1	2
ALPK3	1
CAMK2G	1
CAMKV	2
CDK7	2
DYRK3	1
EGFR	1
EPHA10	1
EYA2	1
HIPK1	2
HIPK2	1
JAK1	1
LATS2	1
MAP3K4	1
MAPK4	1
MAPKAPK5	1
MARK1	1
PLK3	1
PPM1F	1
PPM2C	1
PPP1CC	2
PPP2R1A	3
PPP3CB	1
PPP4C	1
PRKCI	2
PTPN11	1
RIOK1	2
RIOK2	1
SKIP	1
SNF1LK2	1
SYNJ1	1
TRIB1	1

Table S2. Primers used.

hMECP2_qRT_f	GATCAATCCCCAGGGAAAAGC
hMECP2_qRT_r	CCTCTCCCAGTTACCGTGAAG
hGAPDH_qRT_f	CGACCACTTTGTCAAGCTCA
hGAPDH_qRT_r	TTACTCCTTGGAGGCCATGT
hPPP2R1A_qRT_f	ACATGCTACCCACGGTTCTG
hPPP2R1A_qRT_r	ACTCTGCAAGGTGCTGTTGT
hRIOK1_qRT_f	GGCCATGAATGCCCAACAAG
hRIOK1_qRT_r	GTGCAGGGACCTTCTGAACT
hHIPK1_qRT_f	TCCGAAGTGACACTGATGAGG
hHIPK1_qRT_r	GACCTTGGCTTCAGTCCAGA
hHIPK2_qRT_f	ACTGTCCACAACCAGCCCTC
hHIPK2_qRT_r	AATCTGGGCTGTTCCTGTCTG
mGAPDH_qRT_f	AAGGGCTCATGACCACAGTC
mGAPDH_qRT_r	CAGGGATGATGTTCTGGGCA
mPPP2R1A_qRT_f	CTGGACAGCTTGGTGTGGAA
mPPP2R1A_qRT_r	GCAGCCTCACGGATAGCATA

Table S3. shRNAs used.

Source	Clone ID	Gene		shRNA Sense Sequence
Open Biosystems	V2LHS_197495	PPP2R1A	a	GTGGAGTTCTTTGATGAGA
Open Biosystems	V2LHS_198701	PPP2R1A	b	CTGGCTTGTGGATCATGTA
Open Biosystems	V3LHS_641048	PPP2R1A	c	ACCTTGCAGAGTGAAGTCA
Open Biosystems	V2LHS_1799	HIPK1	a	GACAGAGTAGCAACGACAA
Open Biosystems	V2LHS_1805	HIPK1	b	CGCACCACATCTTCTTATA
Open Biosystems	V2LHS_140675	HIPK1	c	CTCCTGCAGTGGAGCATAT
Open Biosystems	V2LHS_261889	HIPK2	a	GAGTCAGTATCCAGCCCAA
Open Biosystems	V2LHS_119612	HIPK2	b	GAGGTGAAATGACTTATTA
Open Biosystems	V2LHS_224550	HIPK2	c	GTCGTGTGCTTCTAAATTA
Open Biosystems	V2LHS_117526	RIOK1	a	CAAATAGAATGAGAACCAT
Open Biosystems	V2LHS_117527	RIOK1	b	CATCTGAGGTCATCTGATT
Open Biosystems	V2LHS_117524	RIOK1	c	GTGTTTAAGCGAGCATATA
RNAi Consortium	TRCN0000012624	Ppp2r1a		GCACCGAATGACTACACTCTTA
N/A	N/A	Scrambled		ATCTCGCTTGGGCGAGAGTAAG